Arabian Journal for Science and Engineering (2019) 44:8361–8376
https://doi.org/10.1007/s13369-019-04096-y

RESEARCH ARTICLE - CIVIL ENGINEERING

Mechanical Characterization of Concrete Reinforced with Different Types of Carbon Nanotubes

A. Hawreen[1,2] · J. A. Bogas[1] · R. Kurda[1,2]

Received: 15 February 2019 / Accepted: 5 August 2019 / Published online: 19 August 2019

Abstract
The main purpose of this study is to characterize the mechanical properties of concrete reinforced with carbon nanotubes (CNT). For this, an extensive experimental program was carried out involving the production and characterization of concrete mixes with five types of CNT, in terms of flexural, splitting tensile and compressive strength, ultrasonic pulse velocity, elastic modulus and fracture toughness. The dispersion ability of CNT in a wide range of pH aqueous suspensions was evaluated prior to their incorporation in concrete. It was found that 0.05–0.1% of CNT were effective to improve all tested properties, increasing the compressive, flexural and splitting tensile strength, as well as the fracture energy and elastic modulus up to 23%, 18%, 27%, 42% and 15%, respectively. The CNT showed great potential to improve the crack resistance and the fracture toughness of concrete, especially in the pre-peak performance of concrete. In relative to other types of CNT, concrete containing higher dosages of lower aspect ratio CNT had the highest improvement of mechanical strength. This is explained by the lower structural damage and higher dispersion capacity of this type of CNT in high pH environments. Nevertheless, higher aspect ratio CNT showed better contribution for the fracture energy, due to their more efficient bridging effect.

Keywords Carbon nanotube · Concrete · Elastic modulus · Ultrasonic pulse velocity · Fracture toughness · Mechanical strength

1 Introduction

Concrete can be characterized at multiple length scales (nano, micro and macro). The behaviour of each scale originates from that at smaller scale. This is where nanoscience has a major role to develop concrete with improved properties. Research on concrete nanotechnology became more interesting after realizing that the chemical and physical properties of cement hydration products are flexible for manipulation, aiming to output a stronger and more durable composite. In these terms, carbon nanotubes (CNT) with their high surface area and extraordinary physical and mechanical properties became promising candidates for composite materials [1, 2]. The aspect ratio over 1:1000 tensile strength up to 60 GPa and modulus of elasticity of about 1 TPa are some of the outstanding characteristics reported for CNT [3, 4].

Cement-based materials (CBM) are characterized by low tensile strength and limited strain capacity, which causes the easy generation and propagation of cracks. The cracking process of concrete starts with separated nanocracks, which later combine to compose microcracks and then macrocracks. Thus, nanosize cracking has a high influence on the composites' performance, in terms of mechanical and durability behaviour. This fact promoted using nanosized fibres for concrete reinforcement to control the nanocrack propagation into larger microcracks. Various researchers have focused on the strengthening of CBM with CNT [5–16]. Generally, CNT's contribution in the nanoscale reinforcement of CBM through the following factors are: filler action, leading to denser CBM; inhibition of crack growth and propagation (CNT's bridging

✉ A. Hawreen
hawreen.ahmed@ist.utl.pt

J. A. Bogas
abogas@civil.ist.utl.pt

R. Kurda
rawaz.kurda@tecnico.ulisboa.pt

[1] CERIS, DECivil, Instituto Superior Técnico, Universidade de Lisboa, Av. Rovisco Pais, 1049-001 Lisbon, Portugal

[2] Department of Civil Engineering, Technical Engineering College, Erbil Polytechnic University, Kurdistan Region, Erbil, Iraq

effect); enhancement of the aggregate-paste interface quality; better stress transfer between cement compounds; better development and distribution of hydrated products (CNT's nucleation effect) [6, 7, 13, 14].

Various researchers (e.g. [6–8, 11–15]) investigated the mechanical strength and microstructure of CNT-cement pastes or mortars. It has been demonstrated that the crack-bridging behaviour of CNT can lead to improvements in the fracture toughness, splitting tensile strength ($f_{ctm,sp}$), compressive strength (f_{cm}), flexural strength ($f_{ctm,fl}$) and modulus of elasticity (E_{cm}).

Cwirzen et al. [11] and Kumar et al. [12] showed that the addition of CNT could lead up to 50% and 36% increase in f_{cm} and $f_{ctm,sp}$, respectively, when cement pastes with different w/c, CNT concentrations and CNT dispersion methods were tested. However, Kumar et al. [12] found that the incorporation of more than 0.5% CNT led to strength reduction. Li et al. [15] studied the $f_{ctm,fl}$ and f_{cm} of mortars with 0.5% functionalized CNT and found 25% and 19% increment, respectively. Musso et al. [13] prepared cement pastes with 0.5% functionalized, annealed and pristine CNT. The rupture modulus of nanocomposites with annealed and pristine CNT was, respectively, 9% and 34% higher than that of the plain paste. The hydrophilic functionalized CNT led to 61% lower strength, causing the absorbance of water available in the mix and preventing the proper hydration of cement paste.

Stynoski et al. [16] studied the fracture toughness and E_{cm} of mortars with 0.125% CNT, 5% silica fume and 0.855% carbon fibres. The authors reported up to 21% and 52% increase in the E_{cm} and crack mouth opening displacement of reinforced mortars. Hawreen et al. [8] also found up to 65% and 54% improvement in the fracture energy and fracture load of CNT-mortars, respectively, when 0.05–0.1% of various types of CNT were incorporated.

Nochaiya and Chaipanich [14] showed that the porosity of cement pastes slightly reduces with the incorporation of CNT. The total measured porosity was 27%, 26% and 23%, in cement pastes with 0%, 0.5% and 1% of CNT, respectively. Li et al. [15] also found a similar trend when 0.5% of functionalized CNT was added. According to Nochaiya and Chaipanich [14], CNT tended to mainly decrease the mesopores (< 50 nm) of cement composites, while macropores (> 50 nm) were little affected.

Hawreen et al. [6, 7], Makar et al. [17] and Makar and Chan [18] studied the CNT's influence on the cement pastes' hydration process, using Vickers hardness test, microscopic analysis, thermogravimetric analysis, Fourier-transform infrared spectroscopy and X-ray diffraction. The authors confirmed the accelerated hydration and early strength improvement in reinforced cement pastes, which was related to the "nucleation effect" formed by CNT, and the adequate bonding between the CNT and the cement compounds.

In short, different trends were reported in the literature, depending on various factors, including the concentration, dispersion technique, type and aspect ratio of CNT, as well as the characteristics of the surrounding matrix and testing procedure. Therefore, the mechanical behaviour of CNT-reinforced CBM is still not well-understood and further research is needed. In addition, most research works have studied the effect of incorporation of CNT on the properties of mortars or cement pastes [6–8, 11–19], and only a few studies were focused on CNT-concrete, namely concerning the steel–concrete bond strength [9], long-term deformation [5] and durability of CNT-reinforced concrete [10].

As shown above, a comprehensive study involving the mechanical characterization of concrete strengthened with different types of CNT has not been published yet. Thus, as a novelty, this study aims to deeply investigate the effect of various types and amounts of CNT on the mechanical properties of concrete, including f_{cm}, E_{cm}, $f_{ctm,fl}$, $f_{ctm,sp}$, ultrasonic pulse velocity (UPV) and fracture toughness. Results are also connected with the characterization of the dispersion efficiency of CNT in aqueous suspensions.

2 Experiments

2.1 Materials

Cement type I 42.5R [20] and two types of fine and coarse aggregates were used to produce concrete (Table 1). For low w/c concrete, superplasticizer (SP) was also used.

Five types of multi-walled carbon nanotubes with different characteristics were chosen from *Timesnano* (Table 2). CNTSL and CNTSS, having high and low aspect ratios, were supplied in aqueous suspension with 5% and 9% weight concentrations, respectively. Dispersion of these two types of CNT was attained with TNWDIS, a polyethylene glycol aromatic imidazole agent. Pure CNTPL has the same aspect ratio of CNTSL, but it was delivered in powder. CNTOH and CNTCOOH, also provided in powder, were originally –OH and –COOH functionalized, respectively. Dolapix PC67 (anionic surfactant) was used for the dispersion of powder supplied powder CNT (CNTCOOH, CNTPL, CNTOH).

2.2 Dispersion of Carbon Nanotubes

Prior to concrete mixing, CNTs were dispersed in water. This procedure included sonication for breaking down bundles of CNT and then the addition of the surfactant (Dolapix PC67) to sustain the dispersion stability. The amount of Dolapix PC67 and the sonication time were defined according to a previous study [25]. CNTOH, CNTCOOH and CNTPL were blended with 40% of the mixing water, taking into account the CNT/Dolapix PC67 mass ratio of 1:0.25, 1:0.5

Table 1 Properties of aggregates

Property	FS[a]	CS[b]	FG[c]	CG[d]	Standard
Water absorption 24 h (%)	0.19	0.26	0.5	0.35	BSEN 1097-6 [21]
Oven-dried particle density (kg/m^3)	2605	2624	2646	2683	BSEN 1097-6 [21]
Apparent particle density (kg/m^3)	2618	2642	2698	2709	BSEN 1097-6 [21]
Saturated and surface-dried particle density (kg/m^3)	2610	2631	2665	2693	BSEN 1097-6 [21]
Loose bulk density (kg/m^3)	1569	1508	1309	1346	BSEN 1097-3 [22]
Voids (%)	39.76	34.74	50.53	49.82	BSEN 1097-3 [22]
Shape index category			SI_{20}	SI_{20}	BSEN 933-4 [23]
Los Angeles category			LA_{35}	LA_{30}	BSEN 1097-2 [24]
Size (mm)	0/2	0/4	0/8	4/11.2	–

[a,b,c,d]Fine and coarse gravels (limestone), and fine and coarse sand (siliceous), respectively

Table 2 Characteristics of CNT as supplied

Notation	CNTSS	CNTSL	CNTPL	CNTCOOH	CNTOH
Commercial name	TNIM8	TNIM6	TNIM6	TNIMC6	TNIMH4
Form as supplied	Suspension	Suspension	Powder	Powder	Powder
Purity (%)	> 90	> 90	> 90	> 90	> 90
Outer diameter (nm)	> 50	20–40	20–40	20–40	10–30
Inner diameter (nm)	5–15	5–10	5–10	5–10	5–10
Length (μm)	10–20	10–30	10–30	10–30	10–30
Aspect ratio	~300	~667	~667	~667	~1000
True density (g/cm^3)	~2.1	~2.1	~2.1	~2.1	~2.1
Tap density (g/cm^3)	0.18	0.16	0.16	0.16	0.14
COOH (%)	–	–	–	1.36–1.5	–
OH (%)	–	–	–	–	2.48

and 1:1, respectively. The remaining mixing water (60%) was afterwards used to saturate the aggregates (Sect. 2.3). The powder CNT-Dolapix-water suspensions were stirred magnetically for 4 h and then sonicated for 30 min. CNTSS and CNTSL were already supplied in aqueous suspension, pre-stabilized with the TNWDIS surfactant. In this case, suspensions were only magnetically stirred with the mixing water and sonicated for 45 and 30 min, respectively.

2.3 Concrete Mix Compositions and Specimen Preparation

Concretes were produced with various w/c (0.35–0.55) and cement contents (380–450 kg/m^3) [26]. The consistency of fresh concrete was class S3 (100–150 mm) [26]. Therefore, SP was needed for mixes with low w/c (0.35, 0.45). To analyse the influence of CNT aspect ratio and dispersion technique, various types of CNT were only tested for concrete with w/c of 0.55. The concentration of CNT varied between 0.05% and 0.5%, by cement weight, based on a previous investigation carried out in CNT-cement pastes [6]. Concretes with w/c of 0.45 and 0.35 were only prepared with or without 0.05% CNTPL. Reference concretes (RC) without CNT were also produced for all w/c range. Mix compositions are presented in Table 3.

For the concrete production, all aggregates were initially mixed for 3 min with 60% of the total water. Then, the remaining 40% of mixing water (with or without CNT) and cement were introduced and mixed for more 3 min. Whenever needed, SP was slowly added to the mix after one more minute. The following specimens were prepared for each testing age and concrete composition: three cubic (150 mm) and three cylindrical (Ø150×300 mm) specimens for f_{cm}; three cylindrical specimens (Ø150×300 mm) for E_{cm}; three cubic specimens (150 mm) for UPV; three cylindrical specimens (Ø150×300 mm) for $f_{ctm,sp}$ strength; three prisms (100×100×500 mm) for $f_{ctm,fl}$ strength; three prisms (100×100×350 mm) for fracture toughness. After 24 h, the specimens were placed in a chamber with controlled temperature of 20 ± 2 °C and RH of about 95%, until the testing day.

2.4 Test Procedures

The compressive strength was tested according to BSEN 12390-3 [27], at 7, 28 and 90 days, for a loading rate of

Table 3 Mix design of concretes

Mixes	w/c	CNT		SP *(%)	Mass of materials (kg/m^3)				
		Type	*(%)		Cement	CG	FG	CS	FS
RC(0.55)	0.55	–	–	–	380	710	242	454	303
C(0.55)_SS(0.1)	0.55	CNTSS	0.1	–	380	710	242	454	303
C(0.55)_SS(0.5)	0.55	CNTSS	0.5	–	380	710	242	454	303
C(0.55)_PL(0.05)	0.55	CNTPL	0.05	–	380	710	242	454	303
C(0.55)_PL(0.5)	0.55	CNTPL	0.5	–	380	710	242	454	303
C(0.55)_COOH(0.05)	0.55	CNTCOOH	0.05	–	380	710	242	454	303
C(0.55)_COOH(0.5)	0.55	CNTCOOH	0.5	–	380	710	242	454	303
C(0.55)_SL(0.05)	0.55	CNTSL	0.05	–	380	710	242	454	303
C(0.55)_OH(0.05)	0.55	CNTOH	0.05	–	380	710	242	454	303
RC(0.45)	0.45	–	–	0.5	400	737	250	474	306
C(0.45)_PL(0.05)	0.45	CNTPL	0.05	0.5	400	737	250	474	306
RC(0.35)	0.35	–	–	1	450	755	251	503	265
C(0.35)_PL(0.05)	0.35	CNTPL	0.05	1	450	755	251	503	265

*By weight of cement

13.5 kN/s. Cylindrical specimens from E_{cm} tests were also tested for f_{cm} at 28 days with a loading rate of 10.5 kN/s. The $f_{ctm,sp}$ tests, according to BSEN 12390-6 [28], and the $f_{ctm,fl}$ tests, according to BSEN 12390-5 [29], were carried out at 7, 28 and 90 days, at loading rates of 3.5 and 0.167 kN/s, respectively. The UPV was evaluated according to BSEN 12504-4 [30] at 7, 28 and 90 days, using a non-destructive tester (PUNDIT)/. The static E_{cm} test was carried out according to the specification LNEC E397 [31], at 28 days. The procedure consisted of four loading and unloading cycles, varying the applied stress between 1 MPa and one-third of the f_{cm}. The loading rate was about 0.5 ± 0.01 MPa/s. The E_{cm} was calculated according to Eq. (1), where E_c is the modulus of elasticity (GPa); $\sigma_{i,n}$ is the initial stress of the cycle (MPa); $\sigma_{f,n}$ is maximum applied stress (MPa); $\varepsilon_{i,n}$ is the strain measured for $\sigma_{i,n}$ and $\varepsilon_{f,n}$ is the strain measured for $\sigma_{f,n}$.

$$E_c = \left[\frac{\sigma_{f,n} - \sigma_{i,n}}{\varepsilon_{f,n} - \varepsilon_{i,n}}\right] \times 10^{-3} \quad (1)$$

The toughness test was carried out at 28 days in notched beams under three-point loading, according to ASTM C1609/C1609 M [32] and RILEM TCS [33]. An aluminium plate was fixed on each opposite face of the specimen to hold a deflectometer with 1 µm precision and 25 mm range (Fig. 1). In addition, one clip-on extensometer with similar precision was installed at the notch to monitor the crack mouth opening displacement (CMOD). The deformation rate was 0.05 mm/min. Three different mechanical properties were derived from the toughness test, namely the fracture energy (G_f), Young's modulus (E) and $f_{ctm,fl}$ (σ_i). The

Fig. 1 Fracture toughness test

fracture energy was calculated based on the RILEM recommendations [33], according to Eq. (2).

$$G_f = \frac{A_o + mg\delta_o}{(d - a_o)b} \quad (2)$$

where A_o is the total area of the load–deflection (δ_f) curve (N/m), mg is the beam self-weight (kg), δ_o is the deflection at the failure load (m), d is the beam depth (m), b is the beam width (m) and a_o is the notch depth (m).

The Young's modulus (E) was calculated from Eq. (3) [34], in which C_i is the initial compliance from the load–CMOD curve (m N^{-1}), and S is the span length (m).

$$E = \frac{6 \times S \times a_0 \times V_1(\alpha)}{C_i \times d^2 \times b} \tag{3}$$

In Eq. (3), V_1 and α were calculated according to Eq. (4) and (5), respectively, in which HO is the holder thickness of the clip gauge.

$$V_1(\alpha) = 0.76 - 2.28\alpha + 3.87\alpha^2 - 2.04\alpha^3 + \frac{0.66}{(1-\alpha^2)} \tag{4}$$

$$\alpha = \frac{a_0 + HO}{d + HO} \tag{5}$$

2.5 Characterization of Carbon Nanotube Suspensions

The dispersion capacity of all CNT types in aqueous suspension was characterized prior to their incorporation in concrete. The investigation was carried out for pH values up to approximately 14, simulating the behaviour of CNT in high pH environment, typical of CBM. Thus, the effect of acid functionalization and dispersant type on CNT dispersion in low, neutral and high pH solution was evaluated. The CNT suspensions were analysed regarding particle surface charge, using Malvern-Zeta Sizer Nano-ZS. The magnitude of particle surface charge can be associated with their stability in suspension, since higher surface charges correspond to increased electrostatic repulsion and thus increased stability. On the contrary, suspensions with low Zeta potential values (typically between +25 mV and −25 mV) tend to aggregate due to van der Waals interactions [35]. CNT were mixed with water in a concentration of 0.005%. The dispersion process described in Sect. 2.2 was considered to prepare each CNT suspension. To avoid the effect of foreign ions in the environment ionic force, deionized water was used to prepare the suspensions, at 25 ± 0.2 °C. The suspensions' pH was varied between 2 and 14, using tailored amounts of HCl or NaOH aqueous solutions.

The Zeta potential results are presented in Fig. 2. At low pH (1.9–7), the Zeta potential values of the CNT suspensions decreased with increasing pH. At higher pH values (7–12.5), the curves followed an opposite trend. Most suspensions were leaning towards having constant Zeta potential plateau for pH values between pH 5 and 10, which is also the range where the suspensions had their highest dispersion stability. CNTSS showed the highest Zeta potential in comparison with other CNT types, while CNTSL had the lowest Zeta potentials. This behaviour of CNTSS stands for their better dispersion and higher suspension stability, even at high pH. The CNTs of higher aspect ratio (CNTSL, CNTPL, CNTCOOH and CNTOH) were more prone to agglomerate than CNTSS. For CNTCOOH, CNTOH and CNTPL suspensions with pH of 6 ± 0.1, the Zeta potential corresponded to −38.8, −34.8 and −25.5 mV, respectively. This means that –COOH and –OH functionalized CNT tend to disperse better in water as compared to pure CNTPL, due to their high hydrophilicity. At high pH, the Zeta potential decreased for all solutions, but the relative behaviour between different types of CNT was about the same.

Despite aiming at ideal CNT dispersion in aqueous suspension, care must be taken to reduce the unwanted damage (carbon atomic structure damage, CNT amorphization, CNT length shortening) resulting from the sonication and acid functionalization process. Therefore, balance must be achieved between adequate dispersion and low structural damage of CNT. To analyse the level of damage, Raman spectroscopy was carried out. In fact, the frequency, intensity and shape of Raman vibrations in CNT are related to their morphological and structural features, including structural and lattice defects [36, 37]. The spectra were collected from a micro-Raman spectrometer (HR Evolution, Horiba

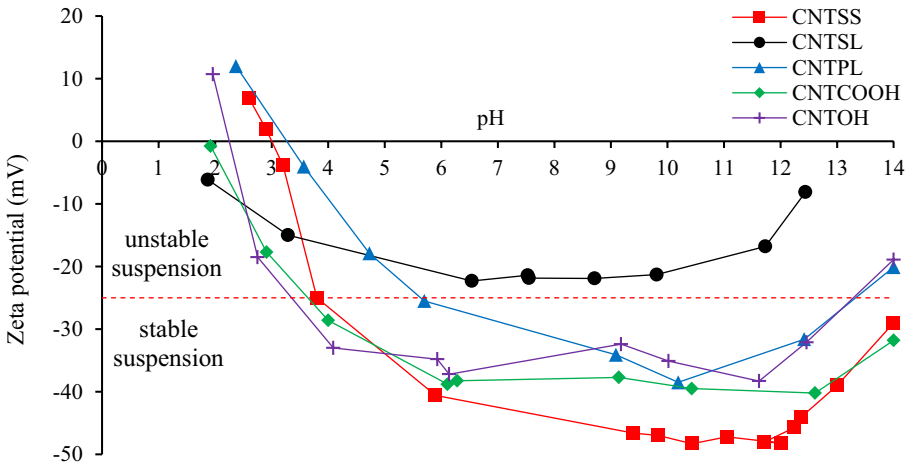

Fig. 2 Zeta potential of different CNT suspensions

Jobin–Yvon), with 532 nm laser, 100 × objective, 5 accumulations and 10 s acquisition. The software Fityk 0.9.8 was used for background removal, and peak fitting was performed using the Lorentzian function. Similar to Zeta potential analysis, the CNT suspensions for Raman spectroscopy were prepared at concentration of 0.005%, following the dispersion procedure described in Sect. 2.2.

All different types of CNT (as supplied) were observed for their peak shape varieties using Raman spectroscopy (Fig. 3a). Normally, the Raman spectrum of carbon materials includes two prominent features, the D peak (I_D) and the G peak (I_G), which are related to the CNT's length and the distance between point defects in the carbon crystallite lattice, respectively [37]. Changes in the G and D peaks denote damage in CNT. Figure 3b presents the influence of the dispersion process (sonication and acid functionalization) on the Raman spectrum of different CNT types. The I_D/I_G ratio is inversely proportional to the CNT's length or to the mean crystallite size in the direction of the plane [37]. Based on the results indicated in Fig. 3b, it can be concluded that the increase in CNT's amorphization features with sonication energy is lower for CNTSS, followed by CNTSL, CNTPL, CNTCOOH and CNTOH. The higher damage in CNTCOOH and CNTOH is related with the functionalization process applied by the supplier. In fact, it is stated that some of the orbital hybridisations of carbon atoms were converted from sp^2 to sp^3 after the acid treatment.

3 Results and Discussion

3.1 Compressive Strength

The mean f_{cm} obtained from cubic ($f_{cm,c}$) and cylindrical ($f_{cm,cyl}$) specimens is presented in Table 4. The f_{cm} of CNT-reinforced concretes relative to the f_{cm} of RC mixes (Δ) is also indicated. In addition, the "coefficients of variation" (CV) are also presented in Table 4. CV of all

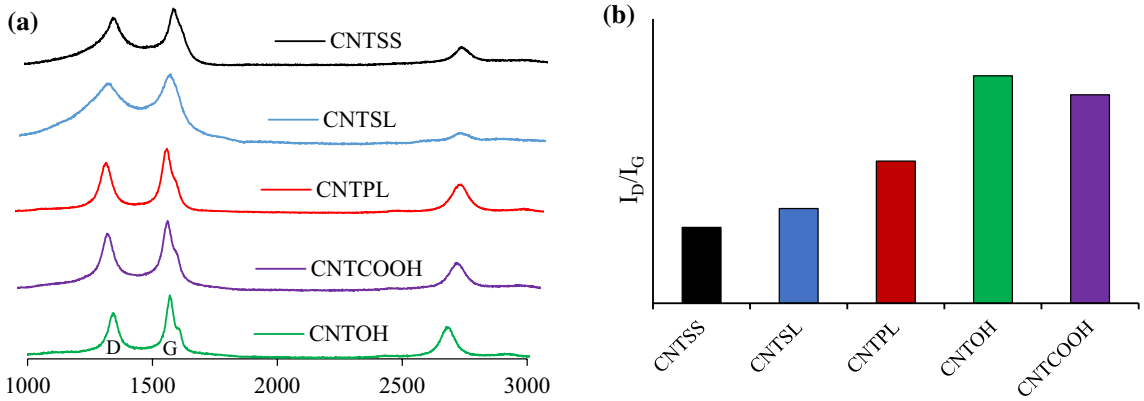

Fig. 3 **a** Raman spectra of CNT, and **b** I_D/I_G ratios of dispersed CNT

Table 4 Compressive strength of concrete cubes ($f_{cm,c}$) and cylinders ($f_{cm,cyl}$)

Mixes	$f_{cm,c}$									$f_{cm,cyl}$		
	7 days			28 days			90 days			28 days		
	MPa	Δ	CV	MPa	Δ	CV	MPa	Δ	CV	MPa	Δ	CV
RC(0.55)	36.8	–	4.6	47.5	–	4.8	54.7	–	3.5	45.4	–	5.6
C(0.55)_PL(0.05)	40.4	9.7	2.5	52.1	9.6	2.3	59.2	8.3	2.6	49.3	8.4	1.4
C(0.55)_PL(0.5)	38.6	4.8	4.1	44.5	−6.3	1.1	53.1	−2.9	0.1	–	–	–
C(0.55)_COOH(0.05)	38.4	4.2	2.4	51.6	8.7	1.6	58.4	6.8	2.8	49.1	8.0	2.2
C(0.55)_COOH(0.5)	41.0	11.4	2.8	47.3	0.4	2.4	55.0	0.6	2.7	–	–	–
C(0.55)_SS(0.1)	45.1	22.5	2.5	57.5	21.0	4.0	66.7	21.8	4.8	55.6	22.3	0.4
C(0.55)_SS(0.5)	38.4	4.1	5.6	51.2	7.8	1.7	57.5	5.1	3.2	48.5	6.8	2.0
C(0.55)_SL(0.05)	35.6	−3.4	7.6	46.2	−2.8	4.0	50.7	−7.3	2.5	45.7	0.7	1.5
C(0.55)_OH(0.05)	40.0	8.5	1.2	50.7	6.7	2.3	59.0	7.9	1.9	49.5	9.0	1.2
RC(0.45)	56.1	–	1.1	64.7	–	2.4	67.8	–	8.1	60.8	–	0.5
C(0.45)_PL(0.05)	55.7	−0.6	1.0	64.0	−1.1	2.2	72.2	6.4	2.1	66.8	9.8	0.1
RC(0.35)	73.6	–	4.0	78.3	–	3.2	85.3	–	2.7	77.5	–	7.2
C(0.35)_PL(0.05)	78.3	6.4	5.1	84.9	8.5	6.1	91.2	6.9	9.2	88.6	14.3	0.3

CNT-reinforced concretes were similar to RC, except those with w/c of 0.35, being lower than 4%, which are in accordance with BSEN 12390-3 [27]. The results show that the reinforcement efficiency depends on the type and quantity of CNT and also on the w/c ratio. For example, the f_{cm} increase in CNT-concretes was as high as 22% at 28 days, confirming the contribution of CNT for the strength improvement of CBM. This general improvement is essentially related to the effects of nucleation, filler and bridging [6, 7, 10]. Only the incorporation of CNTSL and high quantities of CNT (0.50%) of greater aspect ratio were not effective. As discussed in Sect. 2.5 (Fig. 2), it was harder to disperse high aspect ratio CNT, when the commercial surfactant was adopted (CNTSL). The higher aspect ratio and surface area of CNTSL enhance the attraction forces between nanotubes and promotes the tangle effect between them.

Compared to cement pastes [6] and mortars [8], from previous studies of the authors, the strength increment provided by the same amount and type of CNT was lower in reinforced concretes. The main difference between mortars and concretes is the size of the aggregates, in which larger aggregates will affect the CNT dispersion in the cementitious matrix and the failure mode. On the one hand, it is more difficult to ensure an appropriate CNT dispersion during concrete mixing, which may result in poorer dispersibility. On the other hand, apart from the cement paste, the interface transition zone (ITZ) also influences the mechanical behaviour of concrete. In this case, a lower strength improvement can mean that CNT should not considerably improve the ITZ quality of the aggregate-paste. Figure 4 shows one example of the f_{cm} failure of concrete with w/c of 0.35 and 0.05% CNTPL. For this high-strength concrete, the failure path travelled through the aggregates in various regions of the specimen. Therefore, the CNT incorporation, at least, did not negatively affect the aggregate-paste bond and the concrete strength was not significantly affected by the ITZ. According to Kowald and Trettin [38], the CNT may contribute to decrease the crystalline $Ca(OH)_2$ content in the ITZ. Therefore, as this type of $Ca(OH)_2$ contributes to the strength reduction and higher permeability of concrete [39], the CNT incorporation may have a beneficial effect in these regions. Nevertheless, whether the f_{cm} is influenced by the ITZ or by the aggregate strength, the cement matrix quality assumes less relevance on the concrete strength. Therefore, the CNT reinforcement efficiency would be higher in cement pastes and mortars than in concrete.

The improvement of f_{cm} due to the addition of low amount of CNT suggests their positive effect in the microstructure of concrete (Table 4). However, the strength increase was highly influenced by the type and dispersion technique of CNT. In relative to RC, the f_{cm} increment of concrete with 0.05% of CNTPL, CNTCOOH, CNTOH, CNTSL and 0.1% of CNTSS was 10%, 9%, 9%, 1% and 22%, respectively. These significant differences between CNT-concretes were attributed to three main factors: the CNT aspect ratio (Table 2), the CNT dispersion technique (Sect. 2.2) and the CNT spacing in the matrix [7]. Although the CNT of higher aspect ratio should give better reinforcement capacity and pull-out strength as a result of their improved bridging behaviour, they are more prone to agglomerate, showing lower strength increment in relative to CNT of lower aspect ratio (CNTSS) (Fig. 2).

Fig. 4 Compressive failure of concrete specimen with w/c of 0.35 and 0.05% CNTPL

In a previous study of the authors [7], it was theoretically calculated that CNT of lower aspect ratio may better guarantee the force transfer in microcracks (CNTSS), despite the greater free space between them. Furthermore, experimental analysis carried out in Sect. 2.5 indicated that when compared to other CNT, CNTSS was less damaged after the sonication process (Fig. 3b) and its dispersibility in high pH environments was higher (Fig. 2). This may explain the optimum strength improvement attained in concrete containing CNTSS. The greater dispersion quality of CNTSS has also been shown in microscopic analysis carried out in previous studies with cement pastes and mortars [6–8].

Apart from the aspect ratio, the results show that the reinforcement efficiency of CNT is also influenced by the dispersion technique. For example, concretes with CNTPL and CNTSL showed very distinct results even though they had the same aspect ratio. This behaviour confirms the influence of different dispersion techniques (Dolapix PC67 for CNTPL and TNWDIS for CNTSL), i.e. concrete with CNTPL showed f_{cm} improvements up to 10%, while with CNTSL was as low as − 3%.

Concretes with functionalized CNT (CNTOH and CNT-COOH) obtained higher increments (7–9%) than CNTSL-concretes, but still much lower than CNTSS-concretes, as compared to RC. Even though functionalized CNTs are less prone to agglomerate because of their greater hydrophilicity, which provides a stronger chemical bond with the cementitious matrix, the functionalization process introduces CNT structural defects (Fig. 3b). In addition, the hydrophilic functionalized CNTs demand higher water absorbance, which may hampers the hydration process [13]. According to [7], the functionalized CNT may also decrease the strength of concrete because they promote more ettringite formation [7]. Nevertheless, the strength of concretes with functionalized CNT was similar to that with pristine CNT (CNTPL) of similar aspect ratio.

In accordance with the theoretical study of Hawreen et al. [7], 0.5% of CNT simulates sufficient level of strength reinforcement, compatible to the adequate force transfer between cracks. However, f_{cm} of concrete decreases at high incorporation ratio (0.5%), regardless of the CNT type (Table 4). In fact, concretes with 0.5% CNTSS had about 12% lower f_{cm} when compared to concretes with only 0.1% CNTSS. The addition of 0.5% of CNTCOOH and CNTPL even led to f_{cm} decrements up to 6%, as compared to RC. The inefficiency of these concrete reinforcements was related to the lower dispersion of CNT when high amount was incorporated [7]. Predictably, the incorporation of high amounts of longer CNT (CNTCOOH, CNTPL) decreased f_{cm} more than short CNT (CNTSS). This shows that the effect of CNT agglomeration on f_{cm} is proportional to both amount of CNT and its aspect ratio.

For a certain amount and type of CNT, the strength improvement appeared to be influenced by the w/c (Table 4). Regarding the cylindrical specimens, the f_{cm} improvement increased with decreasing w/c. This may be related to the addition of SP in low w/c concrete, which helped further dispersion of CNT. In addition, for the same volume of paste, concrete mixes with low w/c (0.35) had a higher amount of CNT (% of cement weight). However, the same trend was not confirmed in cubic specimens, where in general the CNTs were less effective in low w/c concrete. The higher efficiency of CNT in cylindrical specimens can be associated with the drying conditions suffered by these samples, which were only tested after the tests of E_{cm}. In this case, shrinkage cracks were developed and CNTs could better contribute by their bridging effect in the matrix reinforcement. Nevertheless, this does not explain the very low effectiveness shown by concrete with CNTPL and w/c of 0.45 in cubic specimens. This may be related with the unexpected high strength obtained for RC (0.45). Also note that, in some cases, the small differences between concretes are within the test variability, which makes it complex to accurately interpret the results.

In terms of strength development, the incorporation of CNT in concrete seems to be more efficient at early ages, regardless of the amount and type of CNT and the w/c (Table 4). The exception occurred for w/c of 0.45, which confirms the unexpected values mentioned before. This behaviour was attributed to the positive effect of CNT on the cement hydration at early age. In addition, for concretes at younger ages, the force transmitted between the paste and the CNT is smaller, contributing to a greater effectiveness of the reinforcement system. The greatest reduction in strength was found for concretes reinforced with high dosages (0.5%) of CNTCOOH and CNTPL. The f_{cm} changed by 11%, −6% and −3%, at 7, 28 and 90 days, respectively, was compared to reference concrete. The greater content of CNT and surfactant should have assisted the faster cement hydration, due to the nucleation effect and better distribution of cement particles. However, at later phases, the worse uniformity attained in these CNT-concretes [7] was apparent and the strength was even lower than that of RC.

3.2 Modulus of Elasticity

In general, the incorporation of CNT improves the E_{cm} of concretes (Table 5) due to the retention provided by CNT on microcrack propagation [7] and their effect in nanoporosity reduction [6, 10]. Compared to RC(0.55), the maximum E_{cm} was registered in concrete with 0.10% of CNTSS (15% improvement), followed by those containing 0.05% CNTPL (8%), 0.05% CNTCOOH (5%), 0.05% CNTOH (2%) and 0.05% CNTSL (−3%). These results corroborate the different performances seen in f_{cm} for each CNT type (Sect. 3.1). The addition of high quantities of CNT causes lower E_{cm} increments. For example, when the amount of CNTSS increased from 0.1 to 0.5% the improvement of elasticity modulus decreased from 15 to only 2%. This behaviour confirms the agglomeration effect occurred for high percentages of CNT incorporation [7]. Once more, the addition of 0.05% CNTPL was more relevant in low w/c concrete (0.35), corroborating the obtained results in f_{cm} tests (Sect. 3.1).

The E_{cm} of concrete is essentially influenced by its age, the aggregate-paste ITZ, and the aggregates and cement paste properties [40]. Since CNT can only work in the cement paste (which covers about 30% of the concrete volume), the E_{cm} should not be significantly affected. Nevertheless, an increment of 15% was found in C(0.55)_SS(0.1) mix, as compared to RC(0.55) (Table 5). In addition, the E_{cm} was about 5-8% improved, when CNTPL was incorporated. This shows that CNT can effectively reinforce the cement matrix. Similar behaviour was found in other works carried out in mortars or cement pastes with CNT [6, 8, 16, 41].

The relation between f_{cm} and E_{cm} at 28 days is presented in Fig. 5. The relationship involves 11 average results for E_{cm}

Table 5 Elastic modulus (E_{cm}) and ultrasonic pulse velocity (UPV) of concretes

Mixes	E_{cm}			UPV								
	28 days			7 days			28 days			90 days		
	GPa	Δ(%)	CV (%)	km/s	Δ (%)	CV (%)	km/s	Δ (%)	CV (%)	km/s	Δ (%)	CV (%)
RC(0.55)	36.0	–	1.5	4.5	–	1.7	4.7	–	0.6	4.7	–	0.7
C(0.55)_PL(0.05)	37.6	4.6	0.3	4.6	2.3	0.4	4.8	2.3	1.6	4.8	2.1	1.5
C(0.55)_PL(0.5)	–	–	–	4.6	1.9	0.9	4.8	1.4	0.4	4.8	0.9	0.8
C(0.55)_COOH(0.05)	37.6	4.5	0.8	4.5	−0.3	2.1	4.7	1.0	0.8	4.8	0.6	1.2
C(0.55)_COOH(0.5)	–	–	–	4.7	2.8	0.4	4.8	1.7	0.5	4.8	2.0	1.0
C(0.55)_SS(0.1)	41.2	14.5	0.6	4.6	2.5	1.7	4.8	2.6	0.6	4.9	2.8	1.2
C(0.55)_SS(0.5)	36.6	1.9	1.2	4.6	1.6	0.7	4.7	1.1	0.3	4.7	0.5	0.6
C(0.55)_SL(0.05)	34.9	−2.9	1.3	4.3	−4.7	0.3	4.4	−7.1	0.8	4.4	−5.9	1.8
C(0.55)_OH(0.05)	36.5	1.5	1.0	4.6	0.6	2.3	4.7	0.2	0.5	4.7	−0.6	1.6
RC(0.45)	41.0	–	2.0	4.8	–	1.2	4.9	–	0.5	4.9	–	1.4
C(0.45)_PL(0.05)	43.4	6.0	1.4	4.8	0.1	1.3	4.9	1.0	0.7	4.9	0.5	1.6
RC(0.35)	47.1	–	0.6	5.0	–	0.4	5.1	–	1.1	5.1	–	1.2
C(0.35)_PL(0.05)	50.9	8.1	1.3	5.1	1.7	0.8	5.1	0.8	0.7	5.1	0.8	1.4

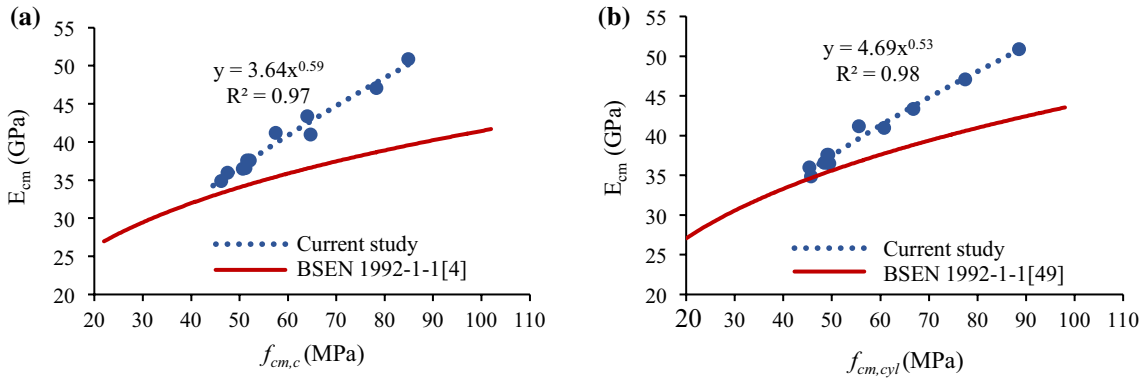

Fig. 5 Relationship between E_{cm} and f_{cm} of **a** cubic and **b** cylindrical concrete samples

between 35 and 51 GPa, $f_{cm,c}$ between 46 and 85 MPa and $f_{cm,cyl}$ between 45 and 89 MPa. As expected, a reasonable correlation was found between these properties ($R^2 > 0.97$).

The E_{cm} usually relates with f_c according to equations of the type $E_{cm} = a \times f_{cm'cyl'}{}^{b}$, where b varies between 1/3 and 1/2 [42]. In this case, Eqs. (6) and (7) were obtained considering the values of Fig. 5. Figure 5b also presents the curve suggested in BSEN 1992-2 [43]. In general, it is concluded that the E_{cm} is slightly underestimated by the normative expression, especially for high-strength concrete.

$$E_{cm} = 4.69 \times f_{cm,cyl}^{0.53}; \quad R^2 = 0.98 \tag{6}$$

$$E_{cm} = 3.64 \times f_{cm,c}^{0.59}; \quad R^2 = 0.97 \tag{7}$$

3.3 Ultrasonic Pulse Velocity

The UPV of materials essentially depends on their stiffness and density. Therefore, a good correlation is expected to be found between UPV and these two properties. Since the density has undergone minor variation between different compositions (±5%), and the E_{cm} was only slightly higher in CNT-reinforced mixes (Table 5), and small differences of UPV were also expected between concretes. The values in Table 5 confirm that the UPV only slightly varied between concretes with distinct CNT types, with variations lower than ±3%. The same hierarchy found in E_{cm} and f_{cm} for each type of CNT was also obtained in UPV. In fact, the highest UPV was attained in CNTSS-concrete, followed by CNTPL.

The increase in UPV in CNT-reinforced concrete was much less significant than that of f_{cm} or E_{cm}. Two factors

may be attributed to these results: UPV varies with the square root of the elasticity and density [44], and therefore it is less sensitive to small variations in the characteristics of cement paste; UPV is evaluated in uncracked samples with a minor contribution of CNT in microcrack propagation. Therefore, the UPV test was less adequate to distinguish the different behaviours of CNT-reinforced CBM.

Taking into account concretes with distinct types and contents of CNT, testing ages (7-90 days) and w/c ratios, a good correlation was obtained between UPV and hardened density (Fig. 6a). This is easily explained since UPV is directly related with density [44] and both properties were not significantly affected by the CNT type. However, a poorer correlation was found between UPV and f_{cm} (Fig. 6b), because strength is essentially controlled by the cement paste, which is significantly affected by the CNT type (Sect. 3.1), contrary to UPV. It is thus shown that UPV is not adequate to estimate the mechanical behaviour of CNT-reinforced concrete.

3.4 Splitting Tensile Strength

The $f_{ctm,SP}$ results are presented in Table 6. In general, CV was lower than 5%, except for some mixes with CNT, especially at 7 days. Since the fracture involves only one section of the cylindrical specimen, defined by the plane along its generatrix (Sect. 2.4), the variability of this test tends to be high. In other words, the tensile strength essentially depends on the composition of concrete in the plane of failure, which may vary between different specimens. Although the variability tended to be higher in CNT-concretes than in RC, it is not possible to conclude about the higher variability of CNT-reinforced concrete. Nevertheless, a poor dispersion of CNT may contribute to a greater variability of this test. In this case, concrete with CNTSS showed CV values lower than 3, confirming the good dispersion ability found in Sect. 2.5.

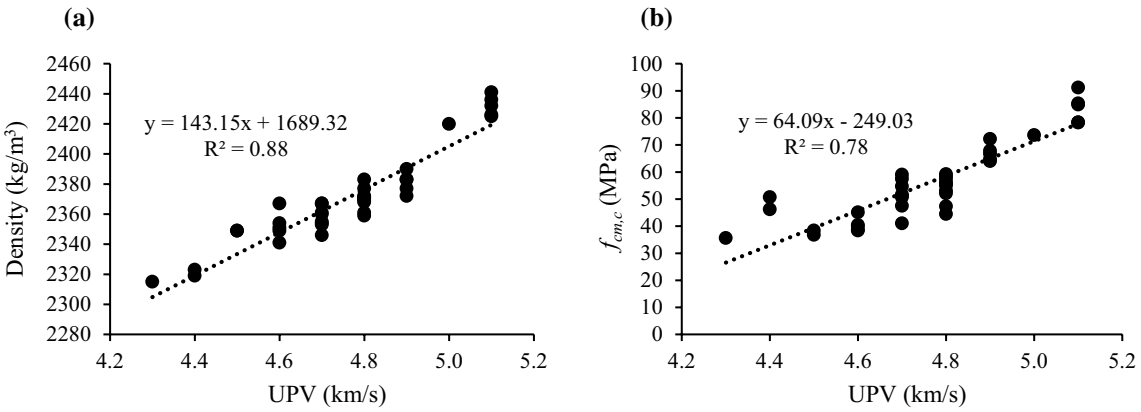

Fig. 6 Relationship between UPV and **a** hardened density or **b** f_{cm}

Table 6 Splitting tensile strength ($f_{ctm,sp}$) of concretes

Mixes	$f_{ctm,SP}$								
	7 days			28 days			90 days		
	MPa	Δ (%)	CV (%)	MPa	Δ (%)	CV (%)	MPa	Δ (%)	CV (%)
RC(0.55)	2.8	0.0	2.0	3.4	0.0	0.0	3.9	0.0	2.0
C(0.55)_PL(0.05)	3.1	11.8	10.0	3.8	12.6	5.0	4.3	10.3	2.0
C(0.55)_PL(0.5)	3.3	20.2	1.0	3.5	3.5	19.0	4.0	2.1	2.0
C(0.55)_COOH(0.05)	3.1	10.7	10.0	3.6	4.1	1.0	3.8	−3.5	2.0
C(0.55)_COOH(0.5)	2.8	1.8	7.0	3.0	−12.2	3.0	3.4	−13.8	1.0
C(0.55)_SS(0.1)	3.2	15.8	3.0	3.9	14.1	2.0	4.4	13.5	1.0
C(0.55)_SS(0.5)	2.9	6.6	2.0	3.5	1.2	2.0	4.2	7.9	2.0
C(0.55)_SL(0.05)	2.6	−6.9	10.0	3.3	−2.0	0.0	4.0	3.6	2.0
C(0.55)_OH(0.05)	2.7	−3.3	2.0	3.5	1.6	3.0	3.6	−7.8	5.0
RC(0.45)	3.3	0.0	16.0	4.1	0.0	1.0	4.6	0.0	2.0
C(0.45)_PL(0.05)	3.6	9.2	22.0	4.4	5.5	9.0	4.8	4.2	2.0
RC(0.35)	4.1	0.0	12.0	4.9	0.0	5.0	5.5	0.0	1.0
C(0.35)_PL(0.05)	5.2	27.1	7.0	5.7	16.5	12.0	6.0	9.1	1.0

The overall results show the ability of CNT to enhance the $f_{ctm,sp}$ of concretes. This behaviour was attributed to the crack retention provided by CNT. The nanotubes are able to anchor the neighbouring C-S–H clusters and bridge the voids between them, which is highly controlled by the CNT's aspect ratio and dispersion technique [7]. Table 6 shows very different reinforcement efficiencies, depending on each studied composition with a given amount and type of CNT. The increment of $f_{ctm,sp}$ in CNT-concretes was as high as 27% at 7 days to as low as −14%, for 0.5% CNT-COOH-concrete at 90 days.

The $f_{ctm,sp}$ was greatly affected by the properties of the CNT (Table 6). Similarly to what was found for other mechanical properties, the highest strength increase at 28 days in concrete with w/c of 0.55 was obtained for 0.10% CNTSS (14% improvement), followed by the mixes with 0.05% CNTPL (13%). The remaining CNTs were almost ineffective with increments of 4%, 2% and −2% with the addition of CNTCOOH, CNTOH and CNTSL, respectively. Once more, the lower aspect ratio CNTSS was the most effective reinforcement, confirming their lower tendency to agglomerate. Similar to f_{cm} results (Sect. 3.1), in general, the tensile strength of CNT-concretes decreased with increasing the CNT amount from about 0.05–0.5%, regardless of the type of CNT. Again, this behaviour is explained by the greater agglomeration of CNT when higher amounts were incorporated. Noteworthy is the high variability found for concretes with 0.5% CNT, suggesting the worse dispersion attained in CNT.

Concerning concretes with different w/c, the same trend found for f_{cm} (Sect. 3.1) was also confirmed for splitting strength, namely the slight higher increment of tensile strength in reinforced concretes with low w/c. As previously explained, this behaviour could be related to the presence of SP in concretes with low w/c (0.35), which better assisted the CNT dispersion. The unexpected modest increase seen in concrete with w/c of 0.45 corroborates the results of f_{cm}. Also note that the low number of specimens tested per each composition and the high variability of the tensile strength test make it difficult to accurately interpret the results.

As found for f_{cm} (Sect. 3.1), the maximum increment of $f_{ctm,sp}$ was obtained at early ages (7 days) (Table 6). After 7 days, the tensile strength improvement compared to RC progressively decreased up to 90 days. As for the other studied properties, it is shown that the CNT affected the initial cement hydration products' morphology, accelerating the early age hydration process. However, a different trend was found for concrete with 0.05% CNTSL, which was not confirmed in compressive tests. This can be attributed to the inherent variability of these tests, especially for concretes with poor dispersion of CNT, as those produced with CNTSL (Sect. 2.5).

3.5 Flexural Strength

The $f_{ctm,fl}$ results are presented in Table 7. In general, the CV of CNT-reinforced concretes were lower than 5% and similar to those obtained in RC mixes. Therefore, the possible increment of variability due to the eventual CNT agglomeration, as found in splitting tensile tests, was not confirmed in this test. In general, the addition of CNT improved the $f_{ctm,fl}$, corroborating the trends found in previous tests (Sect. 3.1 and 3.4). It is thus confirmed that CNT are potentially able to increase the tensile strength of concrete, which is one of the least positive characteristics of these materials.

Table 7 Flexural strength ($f_{ctm,fl}$) of concretes

Mix	$f_{ctm\,f}$								
	7 days			28 days			90 days		
	MPa	Δ (%)	CV (%)	MPa	Δ (%)	CV (%)	MPa	Δ (%)	CV (%)
RC(0.55)	4.1	0.0	2.0	5.6	0.0	1.9	6.0	0.0	2.3
C(0.55)_PL(0.05)	4.4	7.3	1.9	5.8	2.7	1.8	6.3	5.1	1.3
C(0.55)_PL(0.5)	4.0	−2.4	2.0	5.5	−2.2	3.9	5.9	−1.9	1.4
C(0.55)_COOH(0.05)	4.1	0.0	2.0	5.8	3.7	0.9	6.3	4.5	5.7
C(0.55)_COOH(0.5)	4.0	−2.4	2.0	5.6	0.0	1.5	6.0	0.0	1.4
C(0.55)_SS(0.1)	4.7	14.6	1.7	6.1	9.5	0.8	6.6	10.0	1.2
C(0.55)_SS(0.5)	4.0	−2.4	2.0	5.6	−0.8	0.4	5.7	−5.7	3.3
C(0.55)_SL(0.05)	3.9	−4.9	2.1	5.3	−5.2	3.6	6.3	5.4	1.2
C(0.55)_OH(0.05)	4.0	−2.4	2.0	6.0	6.7	0.4	6.0	−0.1	3.5
RC(0.45)	4.9	0.0	1.7	6.0	0.0	1.0	6.7	0.0	0.8
C(0.45)_PL(0.05)	5.6	14.3	1.5	6.6	11.2	2.0	7.3	8.9	2.7
RC(0.35)	6.1	0.0	1.3	8.5	0.0	3.9	9.2	0.0	0.2
C(0.35)_PL(0.05)	7.2	18.0	1.1	9.7	14.3	1.0	10.0	9.4	2.6

Nonetheless, the improvements of $f_{ctm,fl}$ were modest and depend on the amount and characteristics of CNT. The improvement of $f_{ctm,fl}$ in CNT-concretes varied between 18 and −6%, when compared to RC. On the one hand, the $f_{ctm,fl}$ is influenced by the presence of aggregates [45] and the CNT can only participate in the cement paste. On the other hand, the aggregates negatively affect the uniform dispersion of CNT. Therefore, the contribution and influence of CNT to $f_{ctm,fl}$ should be low. Similar increments of $f_{ctm,fl}$, lower than 10–15%, were reported by other authors, taking into account identical amounts of CNT, either in cement pastes [11] or in mortars [46, 47]. However, other authors documented higher increments, over 30%, especially in cement pastes [13, 41, 48]. In general, we may conclude that regarding the modest increase found in mechanical tests, the addition of CNT in concrete is not yet viable, especially considering the high cost of this material. The total cost of reference concrete in current study was about two times cheaper than reinforced concrete with 0.05% of CNT. As expected, this cost difference increases even more with increasing content of CNT. However, in the last years, the cost of CNT has decreased significantly.

The increase in $f_{ctm,fl}$ was similar to that of f_{cm} (Sect. 3.1) and slightly lower than that found in $f_{ctm,sp}$ (Sect. 3.4), which is better related with the axial tensile strength. The similar behaviour found for tensile and compressive strength is already discussed in Sect. 3.4.

As found for other mechanical properties, it is confirmed that concrete with 0.1% CNTSS attained the highest $f_{ctm,fl}$ improvement at 28 days (9%). For other CNT types, the increment was less than 7%. Moreover, concretes with high aspect ratio CNT and the commercial surfactant (CNTSL) showed even lower $f_{ctm,fl}$ than RC. The poor dispersion attained in these mixes (Fig. 2) was not compensated by the possible reinforced effect provided by CNTSL. As found for f_{cm} (Sect. 3.1) and $f_{ctm,sp}$ (Sect. 3.4), the $f_{ctm,fl}$ decreased with increasing CNT amount, from about 0.05–0.5%, regardless of the CNT type (Table 7).

The same amount and characteristics of CNT had a different effect on the $f_{ctm,fl}$, depending on the w/c ratio. In fact, concrete with low w/c (0.35) showed the maximum $f_{ctm,fl}$ increase (14%) as compared to that of RC (Table 7). Actually, the reinforcement efficiency tended to decrease with the increase in w/c. As discussed before (Sect. 3.1), this behaviour may be attributed to the addition of SP and the higher CNT content per volume of paste in low w/c concretes.

In general, as found in 3.1 (f_{cm}) and 3.4 ($f_{ctm,sp}$), the maximum increase in $f_{ctm,fl}$ was attained at 7 days. Then, the $f_{ctm,fl}$ improvement progressively decreased up to 90 days. The same reasons mentioned for f_{cm} in 3.1 can be attributed.

Taking into account all the expected results obtained in this experimental work for concretes tested at different ages with various w/c ratios and amounts and characteristics of CNT, a good correlation was attained between the tested mechanical strength properties, namely f_{cm}, $f_{ctm,fl}$ and $f_{ctm,sp}$ (Fig. 7). The relationship involved 39 average results for f_{cm} between 36 and 91 MPa, $f_{ctm,fl}$ between 3.9 and 10 MPa and $f_{ctm,sp}$ between 2.6 and 6 MPa. The good correlation was already expected, since both properties were equally affected by the CNT reinforcement and w/c. On average, the $f_{ctm,fl}$ and $f_{ctm,sp}$ were about 11% and 7% of the f_{cm}, respectively. The curve suggested in BSEN 1992-1-1 [49] is also presented in Fig. 7a, assuming that the axial tensile strength is about 90% of the $f_{ctm,sp}$ [49, 50]. It was found that this curve slightly underestimated the $f_{ctm,sp}$ for a given f_{cm}.

A strong relationship was found between $f_{ctm,fl}$ and $f_{ctm,sp}$ (Fig. 7c). According to Canovas [51], the $f_{ctm,sp}$ is 0.5 to 0.7 of the $f_{ctm,fl}$. In this case, the average ratio was 0.52 and the relation was only slightly influenced by the characteristics of CNT.

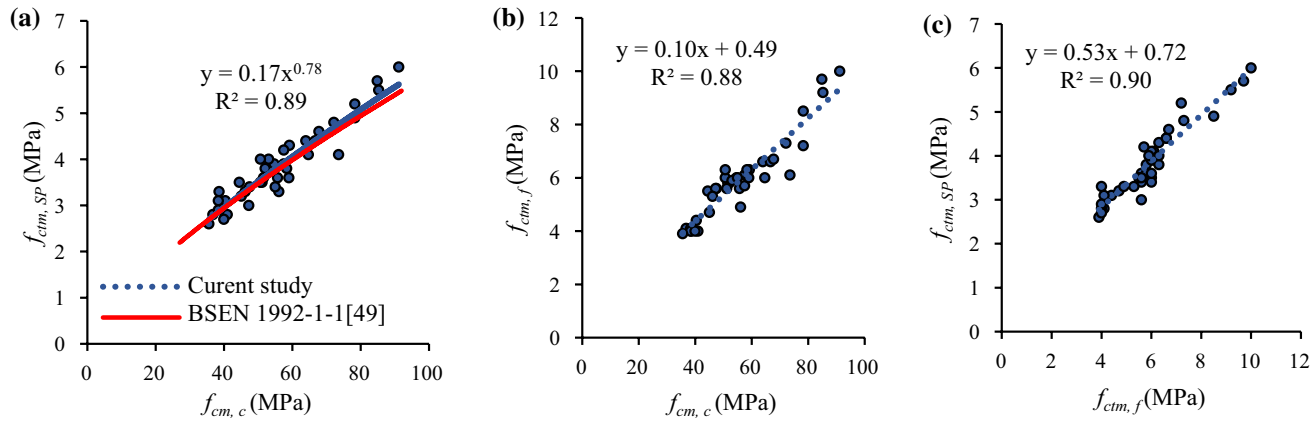

Fig. 7 Relation between the f_{cm} and **a** $f_{ctm,SP}$ and **b** $f_{ctm,fl}$, **c** and between the $f_{ctm,fl}$ and $f_{ctm,sp}$

3.6 Fracture Toughness

The fracture strength (σ_f), fracture energy (G_f) and flexural Young's modulus (E_f) are summarized in Table 8. Since the maximum increase in $f_{ctm,fl}$ and f_{cm} was obtained with the addition of 0.1% CNTSS and 0.05% of the other types of CNT, only these compositions were considered for fracture toughness. Values of CV up to 8% were obtained, due to the high sensitivity of this test to slightly variations on specimen production and test setup, but they were similar for CNT-reinforced concretes and RC.

The average load-δ_f and load-CMOD curves are presented in Fig. 8. The post-peak descending branch of load-δ_f curves was characterized by a progressive drop, typical of brittle materials. Low post-peak deformation was found in concrete mixes with and without CNT (regardless of the CNT type).

The main difference between reinforced and unreinforced concretes concerns the greater contribution of CNT in the pre-peak cracking of concrete, i.e. in the ascending branch of the load-δ_f and load-CMOD curves. Due to their bridging effect, CNT are able to retain the propagation of microcracks and hence the consequent development of macrocracks is delayed. Therefore, CNT-concretes showed lower values of CMOD and δ_f (higher E_f), for a given load, than RC (Fig. 8). However, once the maximum load was attained and macrocracks were developed, CNTs were not able to withstand their suddenly development and an abrupt failure occurred. As shown in previous studies [7, 8], CNT can only contribute with their bridging effect in small microcracks with up to about 1 μm width. Therefore, the hybrid reinforcement of concrete with also micro- and macro-fibres should be the ideal option for the global fracture toughness improvement.

As found for mortars reinforced with similar types of CNT [8], the CNT reinforcement (regardless of their type) was able to increase the toughness of concrete. Compared to RC, the σ_f, G_f and E_f in CNT-concretes increased up to 16%, 42% and 36%, respectively (Table 8). This confirms the high potential of CNT on the cracking resistance improvement of CBM. The increase in fracture energy was lower in CNT-concretes than in mortars, which may be justified by the lower efficiency attained by the CNT in concrete, as discussed in previous points.

The highest fracture energy of concrete with CNT is mainly controlled by the increase in the flexural peak strength. Accordingly, higher residual-strength corresponding to different CMOD and net-deflection are found in CNT-concrete. Comparing to the flexural tests (Sect. 3.5), greater increases of the fracture load were attained in

Table 8 Fracture strength (σ_f), fracture energy (G_f) and flexural Young's modulus (E_f) of concretes

	σ_f			G_f			E_f		
	(MPa)	Δ (%)	CV (%)	(N/m)	Δ (%)	CV (%)	(GPa)	Δ (%)	CV (%)
RC(0.55)	5.5	0	2.4	19.1	0	7.1	38.8	0	2.9
C(0.55)_SS(0.1)	5.7	5.2	4.5	23.0	20.4	8.1	45.2	16.5	0.1
C(0.55)_SL(0.05)	5.3	−2.3	3.8	19.7	3.3	3.7	39.3	1.4	0.1
C(0.55)_COOH(0.05)	6.3	16.2	4.8	26.5	38.8	2.5	52.7	36.1	7.5
C(0.55)_PL(0.05)	5.8	5.6	5.5	27.1	41.9	4.1	49.6	27.9	2.4
C(0.55)_OH(0.05)	6.1	11.1	2.0	20.7	8.5	7.8	45.1	16.3	3.3

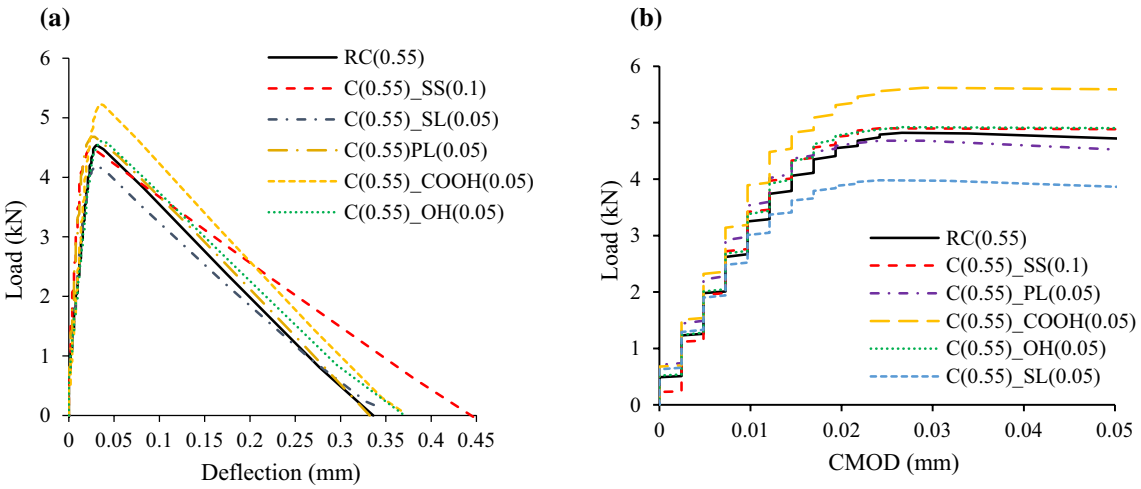

Fig. 8 **a** Load–deflection and **b** load–crack mouth open displacement curves of concretes

CNT-reinforced concretes, which confirms the CNT's ability to enhance the concrete post-cracking behaviour, showing their advantageous action on the crack-propagation retention.

The toughness of reinforced concrete was influenced by the characteristics of CNT. As theoretically explained in a previous study [7] and experimentally showed in Sects. 3.1, 3.2, 3.3, 3.4 and 3.5, CNTSS might better guarantee the transmission of forces throughout microcracks due to their lower aspect ratio, lower structure damage and higher dispersibility in high pH environments. However, the maximum E_f and σ_f were attained in concrete with CNTCOOH, being 17% and 11% higher than that of concrete with CNTSS, respectively. This may be attributed to the covalent bonds between the –COOH and –OH groups of the chemically treated CNT and C–S–H phases of cement matrix [15]. That is, functionalized CNT may provide better bond with the nearby cement hydration products, leading to stronger pull-out resistance and hence better force transfer between cracks. These concretes were followed by those reinforced with the same aspect ratio CNT but without functionalization (CNTPL), with σ_f and E_f being 6% and 28% higher than RC, respectively. Moreover, CNTPL-concrete showed slightly higher G_f improvements (42%) than CNTCOOH-concrete (39%). These results corroborate the somewhat unexpected findings of a previous study with CNT-mortars [7], in which mixes with CNTSS also showed lower fracture energy than those containing higher aspect ratio CNT (CNTCOOH and CNTPL). Therefore, it seems to be confirmed that higher aspect ratio CNT in powder form can provide better crack retention. It is thus concluded that the effect of bridging and the subsequent force transfer throughout microcracks tends to be more effective in reinforced concrete with CNTCOOH and CNTPL. On one hand, high aspect ratio CNTs have bigger surface area/volume ratio, which allow better pull-out tensile strengths and higher strain capacity, leading to more effectiveness in crack retention. On the other hand, functionalized CNTs might also introduce stronger bond with the surrounding cement pastes' hydration products, giving higher pull-out strengths. Nevertheless, this behaviour was not confirmed in the mechanical strength tests, where other factors, such as the filler and nucleation effects, were also important. In such a case, CNTSS might act better, since higher dosages of this CNT type can be easier dispersed in cement matrix than other CNT (Fig. 2). However, in toughness test, the bridging effect looks to be more influential than the other effects of nucleation and filler. In conclusion, depending on the type of CNT, the effects of filler, nucleation and bridging can be more or less relevant. In this case, the well dispersed CNTSS should have contributed more to the former effects and the higher aspect ratio CNT for the bridging effect. In other words, the performance of each type of CNT depends on the relevance of the main contributing effect of CNT in a given property.

The lowest increase in σ_f, G_f and E_f was obtained in concrete reinforced with CNTSL (− 2%, 3%, 1%), followed by CNTOH (11%, 8% and 16%), CNTSS (5%, 20%, 17%), CNTPL (6%, 42%, 28%) and CNTCOOH (16%, 39%, 36%), respectively. Once more, the worst behaviour was found in concretes with CNTSL, evidencing similar values to those of RC. This confirms that the dispersion procedure considered for this CNT type of high aspect ratio was not adequate (Fig. 2). The great difference found between the efficiency of CNTSL and CNTPL, both constituted by CNT of equal morphology, shows the relevance of the CNT dispersion technique on the cementitious composites properties.

4 Conclusions

The effect of different amounts and properties of CNT on the mechanical properties of concrete was studied. The following main outputs were found:

- Suspensions within a wide pH range showed lower dispersion stability in high alkaline environment, similar to that of cementitious matrices. Most stable dispersions were found in the 5–10 pH range. Lower aspect ratio CNT had lower structural damage after sonication and higher dispersion capacity in alkaline environments (high pH) than longer CNT.
- The mechanical strength of concrete was improved by the addition of low amount of CNT, regardless of the characteristics of CNT, w/c and testing age. Only the incorporation of CNTSL was ineffective. However, in general, the mechanical strength improvement was modest. The increment of f_{cm}, $f_{ctm,fl}$, $f_{ctm,sp}$ and E_{cm} was as high as only 20%, 18%, 27% and 15%, respectively. Comparing to mortars and cement pastes, the efficiency of CNT in concrete was less relevant.
- Difference in CNT's properties, amount and dispersion procedure leads to variable concrete performances. Smaller dosages of CNT of lower aspect ratio acted better compared to other CNT. Concretes made with functionalized or pristine CNT did not show significant difference in terms of mechanical strength.
- In general, the CNT-reinforcing efficiency was higher at early ages and decreased with increasing w/c and increasing amount of CNT, from 0.05 to 0.5%.
- Generally, the increase in E_{cm} in concrete containing CNT was only up to about 15%, because this property is more affected by the amount and type of aggregates than by the paste quality.

- Since UPV is essentially affected by the stiffness and density of the material, this property was slightly influenced by the incorporation of CNT (less than 3%).
- Regarding the fracture toughness, the post-peak behaviour was characterized by a progressive drop and the greatest input of CNT occurred at the pre-peak behaviour of concrete. In this region, CNT showed to be able to retain the propagation of microcracks, reducing the CMOD and span deflection for a given load. Increments of up to 16% in the $f_{ctm,fl}$, 36% in the flexural elasticity modulus and 42% in the fracture energy were obtained in CNT-reinforced concretes, confirming the great ability of CNT to improve the microcrack resistance of concrete. The maximum improvements were obtained in concrete with higher aspect ratio CNT, which allows higher pull-outs strengths and hence, more effective crack retention.

Acknowledgements The authors wish to thank research group CERIS for funding the study, as well as the companies BASF and SECIL for supplying the materials used in the experiments. The authors are grateful for the support of Centre for Imaging and Structure of Materials at Aveiro Institute of Materials-University of Aveiro and Department of Physics at Instituto Superior Técnico-University of Lisbon for providing equipment of Zeta potential and Raman spectroscopy tests, respectively. The first author also would like to thank Fundação Calouste Gulbenkian (Portugal) for the financial support through Scholarship No. 125745.

References

1. Avouris, P.; Martel, R.; Derycke, V.; Appenzeller, J.: Carbon nanotube transistors and logic circuits. Phys. B **323**, 6–14 (2002)
2. Yu, M.-F.; Lourie, O.; Dyer, M.J.; Moloni, K.; Kelly, T.F.; Ruoff, R.S.: Strength and breaking mechanism of multiwalled carbon nanotubes under tensile load. Science **287**, 637–640 (2000)
3. Peng, B.; Locascio, M.; Zapol, P.; Li, S.; Mielke, S.L.; Schatz, G.C.; Espinosa, H.D.: Measurements of near-ultimate strength for multiwalled carbon nanotubes and irradiation-induced crosslinking improvements. Nat. Nanotechnol. **3**, 626–631 (2008)
4. Salvetat, J.; Bonard, J.; Thomson, N.; Kulik, A.; Forro, L.; Benoit, W.; Zuppiroli, L.: Mechanical properties of carbon nanotubes. J. Appl. Phys A. **69**, 255–260 (1999)
5. Hawreen, A.; Bogas, J.A.: Creep and shrinkage of concrete reinforced with different types of carbon nanotubes. Constr. Build. Mater. **198**, 70–81 (2019)
6. Hawreen, A.; Bogas, A.; Guedes, M.: Mechanical behaviour and transport properties of cementitious composites reinforced with carbon nanotubes. J. Mater. Civ. Eng. **30**, 04018257 (2018). https://doi.org/10.1061/(ASCE)MT.1943-5533.0002470
7. Hawreen, A.; Bogas, J.; Guedes, M.; Pereira, M.F.C.: Dispersion and reinforcement efficiency of carbon nanotubes in cementitious composites. Mag. Concr. Res. **71**, 408–423 (2019)
8. Hawreen, A.; Bogas, J.A.; Dias, A.P.S.: On the mechanical and shrinkage behavior of cement mortars reinforced with carbon nanotubes. Constr. Build. Mater. **168**, 459–470 (2018)
9. Hawreen, A.; Bogas, J.A.: Influence of carbon nanotubes on steel-concrete bond strength. Mater. Struct. (2018). https://doi.org/10.1617/s11527-018-1279-8
10. Carriço, A.; Bogas, J.A.; Hawreen, A.; Guedes, M.: Durability of multi-walled carbon nanotube reinforced concrete. Constr. Build. Mater. **164**, 121–133 (2018)
11. Cwirzen, A.; Habermehl-Cwirzen, K.; Penttala, V.: Surface decoration of carbon nanotubes and mechanical properties of cement/carbon nanotube composites. Adv. Cem. Res. **20**, 65–73 (2008)
12. Kumar, S.; Kolay, P.; Malla, S.; Mishra, S.: Effect of multiwalled carbon nanotubes on mechanical strength of cement paste. J. Mater. Civ. Eng. **24**, 84–91 (2012)
13. Musso, S.; Tulliani, J.; Ferro, G.; Tagliaferro, A.: Influence of carbon nanotubes structure on the mechanical behavior of cement composites. Compos. Sci. Technol. **69**, 1985–1990 (2009)
14. Nochaiya, T.; Chaipanich, A.: Behavior of multi-walled carbon nanotubes on the porosity and microstructure of cement-based materials. Appl. Surf. Sci. **257**, 1941–1945 (2011)
15. Li, G.Y.; Wang, P.M.; Zhao, X.: Mechanical behavior and microstructure of cement composites incorporating surface-treated multi-walled carbon nanotubes. Carbon **43**, 1239–1245 (2005)
16. Stynoski, P.; Mondal, P.; Marsh, C.: Effects of silica additives on fracture properties of carbon nanotube and carbon fiber reinforced Portland cement mortar. Cem. Concr. Compos. **55**, 232–240 (2015)
17. Makar, J., Margeson, J., Luh, J.: Carbon nanotube/cement composites-early results and potential applications. In: 3rd International Conference on Construction Materials: Performance, Innovations and Structural Implications, Vancouver, pp. 1–10 (2005)
18. Makar, J.; Chan, G.: Growth of cement hydration products on single-walled carbon nanotubes. J. Am. Ceram. Soc. **92**, 1303–1310 (2009)
19. Bogas, J.A.; Hawreen, A.; Olhero, S.; Ferro, A.C.; Guedes, M.: Selection of dispersants for stabilization of unfunctionalized carbon nanotubes in high pH aqueous suspensions: application to cementitious matrices. Appl. Surf. Sci. **463**, 169–181 (2019)
20. BSEN197-1. Cement. Composition, Specifications and Conformity Criteria for Common Cements in BSEN (British Standard European Norm). London, UK (2011)
21. BSEN1097-6. Tests for Mechanical and Physical Properties of Aggregates. Determination of Particle Density and Water Absorption, in BSEN (British Standard European Norm). London, UK (2013)
22. BSEN1097-3. Tests for Mechanical and Physical Properties of Aggregates. Determination of Loose Bulk Density and Voids, in BSEN (British Standard European Norm). London, UK (1998)
23. BSEN933-4. Tests for Geometrical Properties of Aggregates. Determination of Particle Shape. Shape Index, in BSEN (British Standard European Norm). London, UK (2008)
24. BSEN1097-2. Tests for Mechanical and Physical Properties of Aggregates. Methods for the Determination of Resistance to Fragmentation in BSEN (British Standard European Norm). London, UK (2010)
25. Guedes, M., Hawreen, A., Bogas, J., Olhero, S.: Experimental procedure for evaluation of CNT dispersion in high pH media characteristic of cementitious matrixes. In 1º Congress of Tests and Experimentation in Civil Engineering. 4/6/2016. Instituto Superior Técnico, Lisbon, Portugal
26. BSEN206-1. Concrete. Specification, Performance, Production and Conformity, in BSEN (British Standard European Norm). London, UK (2000)
27. BSEN12390-3. Testing Hardened Concrete. Compressive Strength of Test Specimens, in BSEN (British Standard European Norm). London, UK (2009)
28. BSEN12390-6. Testing Hardened Concrete. Tensile Splitting Strength of Test Specimens, in BSEN (British Standard European Norm). London, UK (2009)

29. BSEN12390-5. Testing Hardened Concrete. Flexural Strength of Test Specimens, in BSEN (British Standard European Norm). London, UK (2009)
30. BSEN12504-4. Testing Concrete. Determination of Ultrasonic Pulse Velocity, in BSEN (British Standard European Norm). London, UK (2004)
31. LNECE397. Concretes: determination of the modulus of elasticity under compression. In: LNEC (Laboratório Nacional de Engenharia Civil). Lisbon, Portugal (1993)
32. ASTMC1609/C1609M. Standard Test Method for Flexural Performance of Fiber-Reinforced Concrete (Using Beam With Third-Point Loading) (2012)
33. RILEM-TCS: Determination of the fracture energy of mortar and concrete by means of three-point bend tests on notched beams. Mater. Struct **18**, 285–290 (1985)
34. Shah, S.: Determination of fracture parameters (K_{Ic}^{s} and $CTOD_c$) of plain concrete using three-point bend tests. Mater. Struct. **23**, 457–460 (1990)
35. Lee, J.; Kim, M.; Hong, C.; Shim, S.: Measurement of the dispersion stability of pristine and surface-modified multiwalled carbon nanotubes in various nonpolar and polar solvents. Meas. Sci. Technol. **18**, 3707–3712 (2007)
36. Jiao, L.; Zhang, L.; Wang, X.; Diankov, G.; Dai, H.: Narrow graphene nanoribbons from carbon nanotubes. Nature **458**, 877–880 (2009)
37. Cançado, L.G.; Pimenta, M.A.; Saito, R.; Jorio, A.; Ladeira, L.O.; Grueneis, A.; Souza-Filho, A.G.; Dresselhaus, G.; Dresselhaus, M.S.: Stokes and anti-Stokes double resonance Raman scattering in two-dimensional graphite. Phys. Rev. B. (2002). https://doi.org/10.1103/PhysRevB.66.035415
38. Kowald, T., Trettin, R.: Improvement of cementitious binders by multi-walled carbon nanotubes. In: Bittnar, Z., et al. (eds.), Nanotechnology in Construction 3: Proceedings of the NICOM3, pp. 261–266. Springer, Berlin (2009)
39. Chen, S.J.; Collins, F.G.; Macleod, A.J.N.; Pan, Z.; Duan, W.H.; Wang, C.M.: Carbon nanotube-cement composites: a retrospect. IES J Part A Civ Struct Eng **4**, 254–265 (2011)
40. Neville, A.: Properties of Concrete. Pitman Publishing Comp. Ltd, New York (1995)
41. Zou, B.; Chen, S.J.; Korayem, A.H.; Collins, F.; Wang, C.M.; Duan, W.H.: Effect of ultrasonication energy on engineering properties of carbon nanotube reinforced cement pastes. Carbon **85**, 212–220 (2015)
42. Bogas, J.: Characterization of structural concrete with light aggregates of expanded clay. In: Departamento de Engenharia Civil, Arquitectura e Georrecursos. Ph.D. Thesis. Instituto Superior Técnico (2011) **(in Portuguese)**
43. BSEN1992-2. Eurocode 2. Design of Concrete Structures. Concrete Bridges. Design and Detailing Rules, in BSEN (British Standard European Norm). London, UK (2005)
44. Pundit, Pundit Manual for Use with the Portable Ultrasonic Non-destructive Digital Indicating Tester. C.N.S. Electronics Ltd., London. https://www.sciencedirect.com/science/article/pii/S0041624X12002739#bi0005 (1991)
45. Mehta, P.; Monteiro, P.: Concrete: Microstructure, Properties and Materials. McGraw-Hill Professional Publishing, New York (2006)
46. Manzur, T.; Yazdani, N.: Optimum mix ratio for carbon nanotubes in cement mortar. KSCE J. Civil Eng. **19**, 1405–1412 (2014)
47. Hamzaoui, R.; Guessasma, S.; Mecheri, B.; Eshtiaghi, A.M.; Bennabi, A.: Microstructure and mechanical performance of modified mortar using hemp fibres and carbon nanotubes. Mater. Des. **56**, 60–68 (2014)
48. Kim, H.K.; Nam, I.W.; Lee, H.K.: Enhanced effect of carbon nanotube on mechanical and electrical properties of cement composites by incorporation of silica fume. Compos. Struct. **107**, 60–69 (2014)
49. BSEN1992-1-1. Eurocode 2: Design of Concrete Structures—Part 1-1: General Rules and Rules for Buildings, in BSEN (British Standard European Norm). London, UK (2004)
50. fib10. Bond of Reinforcement in Concrete. Bulletin 10, State-of-Art-Report. Lausanne: fib—CEB-FIP—Fédération internationale du béton, p. 434 (2000)
51. Canovas, M.F.: Colegio de Ingenieros de caminos, canales y puertos: Hormigon. Espanha, Madrid (2004)